Abdominal Radiology

Abdom Radiol (2016)
DOI: 10.1007/s00261-016-0733-8

Performance of diffusion-weighted imaging, perfusion imaging, and texture analysis in predicting tumoral response to neoadjuvant chemoradiotherapy in rectal cancer patients studied with 3T MR: initial experience

Carlo N. De Cecco,[1,2] Maria Ciolina,[1] Damiano Caruso,[1] Marco Rengo,[1] Balaji Ganeshan,[3] Felix G. Meinel,[4] Daniela Musio,[5] Francesca De Felice,[5] Vincenzo Tombolini,[5] Andrea Laghi[1]

[1]Diagnostic Imaging Unit, Department of Radiological Sciences, Oncology and Pathology, I.C.O.T. Hospital, University of Rome "Sapienza" - Polo Pontino, Latina, Italy
[2]Department of Radiology & Radiological Science, Medical University of South Carolina, Charleston, SC, USA
[3]Clinical Imaging Sciences Centre, Brighton and Sussex Medical School, Falmer, Sussex, United Kingdom
[4]Institute for Clinical Radiology, Ludwig-Maximilians-University Hospital, Munich, Germany
[5]Department of Radiotherapy, University of Rome "Sapienza", Rome, Italy

Abstract

Purpose: To determine the performance of texture analysis (TA), diffusion-weighted imaging, and perfusion MR (pMRI) in predicting tumoral response in patients treated with neoadjuvant chemoradiotherapy (CRT).
Methods: 12 consecutive patients (8 females, 4 males, 63.2 ± 13.4 years) with rectal cancer were prospectively enrolled, and underwent pre-treatment 3T MRI. Treatment protocol consisted of neoadjuvant CRT with oxaliplatin and 5-fluorouracile. Unenhanced T2-weighted images TA (kurtosis), apparent diffusion coefficient (ADC), and pMRI parameters (Ktrans, Kep, Ve, IAUGC) were quantified by manually delineating a region of interest around the tumor outline. After CRT, all patients underwent complete surgical resection and the surgical specimen served as the gold standard. Receiver operating characteristic (ROC) curve analysis was performed to assess the discriminatory power of each quantitative parameter to predict complete response.
Results: Pathological complete response (pCR) was reported in six patients and partial response (PR) in three patients. Three patients were classified as non-responders (NR). Pre-treatment kurtosis was significantly lower in the pCR sub-group in comparison with PR + NR ($p = .01$). Among ADC and pMRI parameters, only Ve was significantly lower in the pCR sub-group compared with PR + NR ($p = .01$). A significant negative correlation between kurtosis and ADC ($r = -0.650$, $p = .022$) was observed. Pre-treatment area under the ROC curves (AUC), to discriminate between pCR and PR + NR, was significantly higher for kurtosis (0.861, $p = .001$) and Ve (0.861, $p = .003$) compared to all other parameters. The optimal cutoff value for pre-treatment kurtosis and Ve was ≤0.19 (100% sensitivity, 67% specificity) and ≤0.311 (83% sensitivity, 83% specificity), respectively.
Conclusion: Pre-treatment kurtosis derived from T2w images and Ve from pMRI have the potential to act as imaging biomarkers of rectal cancer response to neoadjuvant CRT.

Key words: Rectal cancer—Magnetic resonance imaging—Texture analysis—Diffusion-weighted imaging—Perfusion imaging—Neoadjuvant chemoradiotherapy

The reported evidence on the role of magnetic resonance imaging (MRI) in predicting and assessing response to neoadjuvant chemoradiotherapy (CRT) in rectal cancer

Correspondence to: Andrea Laghi; *email:* andrea.laghi@uniroma1.it

Journal : 261_ABDI | Dispatch : 4-4-2016 | Pages : 8
Article No. : 733 | ☐ LE | ☐ TYPESET
MS Code : ABDI | ☑ CP | ☑ DISK

are based on classical morphological MR evaluation [1–3]. Novel MR imaging quantitative biomarkers, able to establish more objectively the response to therapy [4–8], can play an important role in the identification of patients with pathological complete response (pCR) after neoadjuvant CRT who might benefit from either less invasive surgical approach (transanal endoscopic microsurgery, TEM) [9, 10] or a "wait-and-watch" strategy [11, 12], or those with good prognosis who might benefit from surgical treatment alone [13, 14], but who are exposed to the long-term toxicity of RT, whereas non-responder along with partial responder might benefit of alternative therapeutical strategies [15, 16].

Different MR imaging biomarkers have been identified in oncologic imaging, namely texture analysis of morphological images, diffusion-weighted imaging (DWI), and perfusion MRI (pMRI).

Texture analysis is a non-invasive method of assessing the heterogeneity within a tumor [17]. Early evidence in literature demonstrated that texture parameters derived from T2w images of rectal cancer have the potential to act as imaging biomarkers of tumoral response to neoadjuvant CRT [18].

There is growing evidence that the use of DWI in association with morphological T2-weighted sequences improves the performance of MRI in the assessment of tumor response after CRT [19, 20] and thus might be also helpful in predicting responders versus non-responders. pMRI is an imaging modality that relies on the dynamic assessment of tracer uptake kinetics [21–23]. A preliminary study on a small cohort of patients has recently demonstrated a correlation between tumor response and K^{trans} in tumor treated with antiangiogenic drugs (Anti-VEGF, vascular endothelial growth factor) [24]. However, the role of pMRI and DWI in pre-CHT evaluation has not been investigated yet.

Therefore, the purpose of this investigation was to determine which one of the quantitative parameters derived from texture analysis, DWI, and pMRI is the most reliable to predict tumor response to neoadjuvant therapy and to evaluate the existing correlation, if any, among these parameters.

Materials and methods

Study population

This prospective study was approved by our institutional ethics committee and all patients gave written informed consent.

12 consecutive patients were prospectively enrolled. All the patients had histologically proved colorectal adenocarcinoma and locally advanced tumor stages II (cT3-4, N0, M0) and III (cT1-4, N+, M0). Exclusion criteria were considered the following: (a) evidence of contraindications to MR examination (e.g., pacemaker, cochlear implant, etc.); (b) incomplete MR acquisition or histopathological analysis; (c) contraindication to the use of neoadjuvant therapy or surgical treatment or suspension of neoadjuvant combination chemotherapy and radiation treatment prior to surgery; (d) hypersensitivity to the study drug or to one of the excipients; and (e) legal incapacity. Patients treated with concurrent and experimental drugs or participation in another clinical trial were also excluded.

Study protocol

All patients underwent 3 MR examinations, as already described in another study [18]. The first MR examination was performed for staging, the second one during the CRT, and the third one at the end of CRT. Between 6 and 8 weeks after the CRT, total mesorectal excision (TME) was performed and one experienced pathologist analyzed the gross specimen.

Due to the specific purpose of this study, we have focused our analyses on pre-treatment MRI examinations for tumor staging and assessment of imaging biomarkers.

MR examination

All MR acquisitions were performed using a 3T scanner (Discovery MR750, General Electrics, Milwaukee, Wisconsin, USA). A routine clinical imaging protocol was performed including high-resolution T2-weighted fast recovery fast-spin echo (2D FRFSE) sequence (TR, 2086-4172 ms; TE, 11.4-122.3 ms; Nex, 2; slice thickness, 4 mm; matrix, 512 × 512) acquired on three standard axis. In addition, dedicated axial oblique and coronal oblique planes were obtained, respectively, orthogonal and parallel to the long axis of the rectum.

For the specific purpose of our study, perfusion imaging (pMRI) and DWI were also added to standard rectal cancer MRI clinical protocol. Axial DWI images were obtained using a single-shot echo-planar imaging sequence with spectral adiabatic inversion recovery fat-saturation technique (TR, 4400 ms; TE, 81.4 ms; Nex, 2; slice thickness, 4 mm; matrix, 256 × 256; *b*-values 0–200–800 s/mm^2), along the three orthogonal directions of the motion-probing gradients. Axial dynamic contrast-enhanced images were obtained using a 3D FSPGR sequence with a volumetric acquisition of the entire rectum which started simultaneously to the IV administration of 2 mL/kg of body weight of gadolinium chelate followed by a 15 mL saline flush at a rate of 2 mL/s. The entire volume was acquired in one second and the acquisition was repeated over a scan time of 60 s using a thin collimation (2 mm) in order to obtain an accurate evaluation of the medium contrast kinetics in the tumoral tissue during all the vascular phases.

Neoadjuvant therapy

Radiation therapy was performed with a 3D-conformational multiple-field technique. A dose of 45 Gy (1.8 Gy × 25 daily fractions over 5 weeks) was erogated to the whole pelvis; in addition, a dose from 5.4 to 9 Gy (1.8 Gy × 3–5 daily fractions) was erogated to the tumor volume, with 6–15 MV energy photons. Chemotherapy was administered through a central venous access, consisting in 2 h of oxaliplatin infusion (50 mg/m^2) for the first day of each week of radiotherapy, plus five daily continuous infusions of 5-FU 200 mg/m^2/die. Patients received 5 or 6 cycles of oxaliplatin, in view of performance status (PS), clinical lymph-nodal involvement, and potential risk of a non-sphincter-conserving surgical procedure. Dose reduction of Oxaliplatin and 5-FU was not planned.

Surgical technique

A standard procedure consisting in TME [25] was performed in all patients by experienced colorectal surgeons with at least 10 years practice in TME procedure.

Histopathological assessment

One experienced gastrointestinal histopathologist performed histopathology analysis by assessing the basic histopathology of the primary tumor (type and grade of the tumor) pre-CRT treatment. A correlation of imaging with pathology of the whole resected irradiated region was also performed examining the intestinal segment harboring the neoplasm by sectioning orthogonal to the long axis, obtaining macrosection specimens of 2–3 mm of thickness. This approach allows preservation of the left–right and antero-posterior orientation of the specimen facilitating the topographic localization of suspect pathological foci seen on MRI. Tumor regression grade (TRG) was assessed by analyzing entirely all specimens. All analyses comprised surgical margins evaluation and other histological features including T stage and N stage following the 7th edition of the American Joint Commission on Cancer. TRG was estimated based on the amount of inflammatory tissue and fibrosis versus the amount of residual viable tumor as follows: grade 0, no regression; grade 1, minor regression (fibrosis ≤25% of dominant tumor mass); grade 2, moderate regression (fibrosis from 26% to 50% of dominant tumor mass); grade 3, good regression (dominant fibrosis >50% of tumor mass); and grade 4, complete regression (fibrotic tissue only with no viable tumor) [26].

Diffusion imaging

Quantitative analysis of DWIs will be performed using the Matlab code (Release 7.10.0, The Mathworks Inc., Natick, MA).

To calculate ADC and diffusion parameters, a region of interest (ROI) is drawn on the rectal cancer on b800 images (mean size 165 mm^2; range, 100–230 mm^2). Then, ROI is transferred to all b-value images using an automated process. Mean signal intensities (SI) are obtained for each ROI with careful exclusion of the necrotic or cystic portions inside the tumor.

Finally, global ADC was calculated from the following equation:

$$S_b/S_0 = e^{-b \times D},$$

using data at *b*-values of 0, 200, and 800 s/mm^2. The Levenberg–Marquardt algorithm was used to perform the mono-exponential fits of ADC.

Perfusion imaging

Perfusion analysis was performed using a two-compartmental model of vascular space (VS) and extravascular/extracellular space (EES). The volume transfer constant between blood plasma and extracellular/extravascular space (K^{trans}, min^{-1}), rate constant between EES and blood plasma (kep, min^{-1}), volume of EES space per unit volume of tissue (Ve), and areas under the concentration curve of Gd contrast agent over 90 s (IAUGC90, mM.s) was calculated from single time–intensity curves derived for each patient from the entire ROI placed on the tumoral lesion. In addition, as tumor enhancement heterogeneity is common, especially after treatment, voxel-wise analysis was performed by deriving these same parameters from the highest 10% (decile) and the highest 25% (quartile) of voxels in the parametric maps. Derived pMRI parameters (K^{trans}, K_{ep}, Ve, and IAUGC90) were recorded for each MR examination (Fig. 1).

Texture analysis

Texture analysis was performed as already described in detail elsewhere [18]. Heterogeneity of rectal tumors was assessed by a single operator (XXX, with 9 years of experience in texture analysis) using a commercially available software (TexRAD Ltd, Somerset, England, UK). A region of interest (ROI) was drawn around the rectal lesion, enclosing only the tumor tissue, at the level of the largest tumor area visualized on the axial T2w MRI images from MR1 and MR2, by an abdominal radiologist (XXX, with 7 years of experience on abdominal MRI), blinded to the histopathological results. Texture analysis comprised an image-histogram technique with an initial image filtration (Fig. 1) followed by quantification of texture within the filtered images. For each patient, texture was measured within the tumor ROI for at the largest cross-section area available. Lesion heterogeneity inside the ROI was

Journal : 261_ABDI | Dispatch : 4-4-2016 | Pages : 8
Article No. : 733 | ☐ LE | ☐ TYPESET
MS Code : ABDI | ☑ CP | ☑ DISK

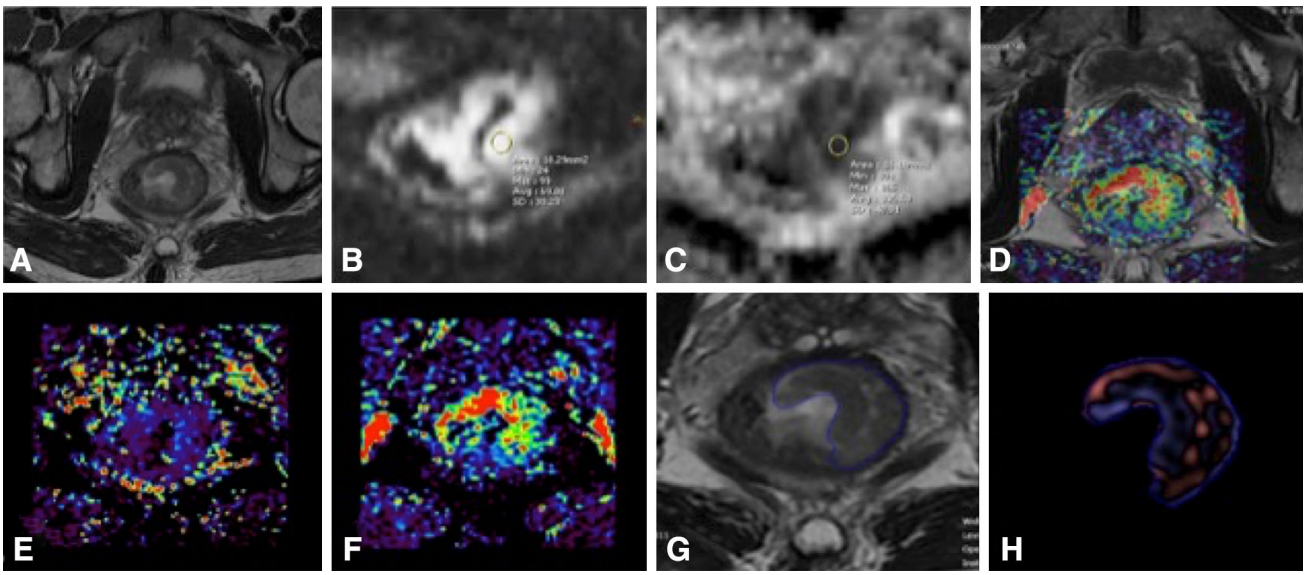

Fig. 1. Multiparametric examination with DWI, pMRI, and texture analysis of a rectal tumor before neoadjuvant treatment. T2-weighted images with the rectal tumor (**A**) and corresponding DWI (**B**) and ADC (**C**); pMRI analysis showing K^{trans} (**D**); Ve (**E**), and IAUGC (**F**) datasets; T2-weighted image (**G**) with corresponding image selectively displaying medium (SSF4) texture image; (**H**) for analysis of the kurtosis.

evaluated with and without image filtration using only kurtosis as histogram parameter. Kurtosis reflects peakedness and tailedness of the histogram; it is related inversely to the number of features highlighted (whether bright or dark) and increases by intensity variations in the highlighted features [27].

The selection of kurtosis and SSF4 was based on the evidence of a recent article showing this combination as the most effective in predicting rectal cancer response to neoadjuvant CRT [18].

Statistical analysis

Statistical analysis was performed by using SPSS (21.0; SPSS, Chicago, IL, USA) and MedCalc version 12.7.2 (MedCalc Software, Ostend, Belgium). Continuous variables are presented as mean ± standard deviation (SD). The Kolmogorov–Smirnov test was used to assess the normal or non-normal distribution of the data. Texture parameters (kurtosis, skewness, MPP) and the response rate among pCR, PR, and NR groups before and after neoadjuvant therapy were compared by using the non-parametric Mann–Whitney *U* test. Relative changes of each parameter were also compared between the different patient subgroups. The presence of a linear correlation among ADC, pMRI parameters, and kurtosis was assessed using Pearson's correlation coefficient. Discriminatory power of texture parameters to predict pCR was assessed by receiver operating characteristic (ROC) curve analysis and the calculated areas under curve (AUC) and the corresponding *p* values. Optimal cutoff values were derived as the cutoff threshold maximizing the Youden's index J, where J = sensitivity + specificity − 1. Sensitivity and specificity were calculated for the determined optimal cutoff values. A *p* value of <0.05 was considered statistically significant.

Results

Patient population

The patient population consisted of 12 patients (8 females, 4 males, median age 64.5 years, range 57–71 years). Median tumor diameter was 23 mm (range 16–50 mm). pCR, partial response, and no response were found in 6, 3, and 3 patients, respectively. Age was lower in the pCR group (median 61.5, range 57–65 years) compared to the PR/NR group (median 68, range 58–71, $p = 0.037$). The tumor diameter was not significantly different between the two response groups ($p = 0.523$).

Baseline kurtosis

Median baseline kurtosis was −0.072 (range −1.252 to 3.074). Baseline kurtosis was significantly different between patients with pCR (median -0.449, range −1.252 to 0.192) and patients with PR/NR (median 0.290, range −0.623 to 3.074) (Fig. 2).

Baseline DWI parameters

Median value of baseline ADC was 0.841 (range 0.715–1.380). There was no significant difference in ADC ($p = 0.818$) between patients with pCR (median 0.926,

Journal : 261_ABDI | Dispatch : 4-4-2016 | Pages : 8
Article No. : 733 | ☐ LE | ☐ TYPESET
MS Code : ABDI | ☑ CP | ☑ DISK

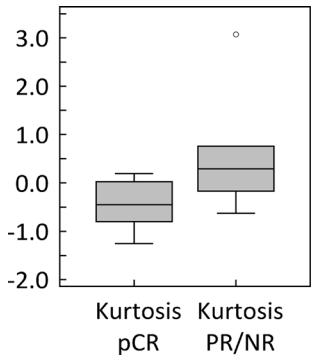

Fig. 2. Baseline Kurtosis was significantly lower in pCR in comparison with PR/NR.

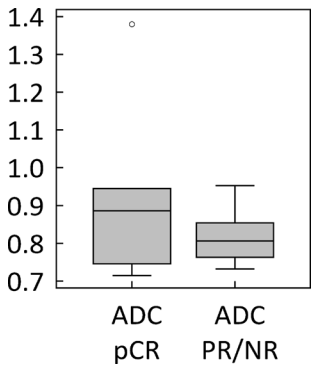

Fig. 3. No significant difference in ADC ($p = 0.82$) was observed between the two groups.

range 0.823–0.988) and patients with PR/NR (median 0.854, range 0.789–0.975) (Fig. 3).

Baseline pMRI parameters

Median values of pMRI parameters were 1.040 (range 0.771–1.327) for Ktrans, 0.678 (range 0.048–2.460) for IAUGC, 0.357 (range 0.108–0.992) for Ve, and 1.683 (range 0.535–8.220) for Kep.

There was no significant difference in IAUGC ($p = 0.310$), Ktrans ($p = 0.689$), or Kep ($p = 0.394$) between the two response groups. Ve was significantly lower in the pCR group (median 0.2775, range 0.108–0.408) compared to the PR/NR group (median 0.5675, range 0.245–0.992, $p = 0.041$) (Figs. 4, 5). Full results are listed in Table 1.

Correlation between baseline kurtosis, ADC, and pMRI parameters

There was no significant correlation between kurtosis and IAUGC ($r = -0.203$, $p = 0.527$), Ktrans ($r = 0.273$, $p = 0.390$), Ve ($r = 0.189$, $p = 0.557$), or Kep ($r = -0.343$, $p = 0.276$). There was, however, a significant negative correlation between kurtosis and

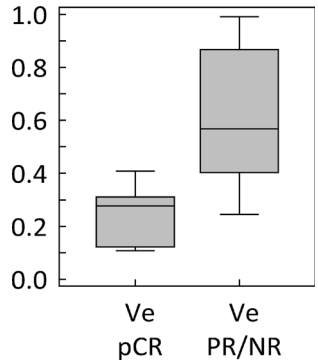

Fig. 4. Ve was the only parameter among in pMRI significantly lower in pCR compared to PR/NR.

ADC ($r = -0.650$, $p = 0.022$) (Fig. 6). Kurtosis also showed a significant positive correlation with patients' age ($r = 0.687$, $p = 0.014$) but not with tumor diameter ($r = -0.242$, $p = 0.473$).

Predictive value of kurtosis, ADC and pMRI parameters

The areas under the receiver operating characteristics curve to discriminate patients with pCR ($n = 6$) from patients with PR/NR ($n = 6$) were 0.861 for kurtosis, 0.694 for IAUGC, 0.569 for Ktrans, 0.861 for Ve, 0.668 for Kep, and 0.556 for ADC. The discriminatory power was significant for kurtosis ($p = 0.001$) and Ve ($p = 0.003$), but not for IAUGC ($p = 0.322$), Ktrans ($p = 0.709$), or ADC ($p = 0.769$). The optimal criteria for the identification of patients with pathological CR were ≤0.192 for kurtosis (100% sensitivity, 67% specificity) and ≤0.311 for Ve (83% sensitivity, 83% specificity) (Fig. 7).

Discussion

The results of our study demonstrate the reliable use of texture analysis based on T2w MR images and pMRI parameters to predict the response of rectal cancer to CRT, in particular differentiating patients with pCR from those with partial response (PR) or non-responders (NR).

Among texture parameters, kurtosis seems to be the best predictor of tumor response. Specifically, we found that pre-treatment kurtosis is the most effective parameter showing a sensitivity and specificity for pCR detection of, respectively, 100% and 67%. Among pMRI parameters, Ve seems to be the most promising parameter, showing a sensitivity and specificity for pCR detection of, respectively, 83% and 83%. Other pMRI parameters (IAUGC, Ktrans, Kep) showed no significant difference between the two patient groups. However, a trend between these parameters and pCR was observed, and increasing the power of our study with

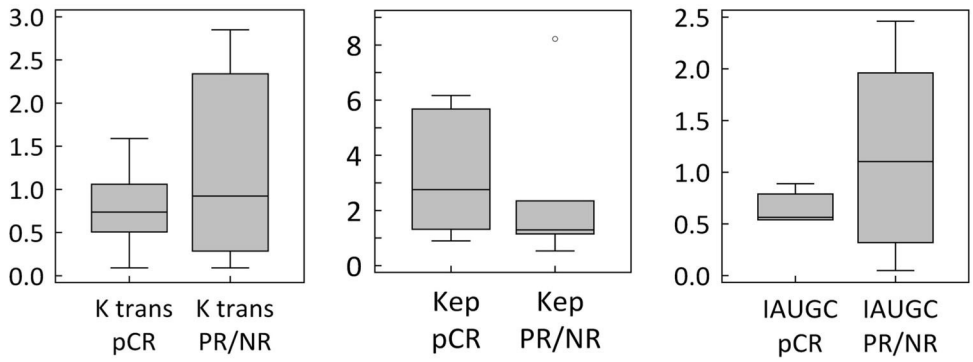

Fig. 5. K^{trans}, Kep, and IAUGC showed no significant difference between the two groups, but a trend was observed.

Table 1. Overall multiparametric results for pCR in comparison with PR/NR

	pCR	PR/NR	*P* value
Kurtosis	−0.45 ± 0.12	0.29 ± 0.09	**<0.001**
ADC	0.88 ± 0.23	0.81 ± 0.25	0.82
K trans	0.69 ± 0.40	0.83 ± 0.34	0.69
IAUGC	0.51 ± 0.19	1.13 ± 0.77	0.31
Ve	0.28 ± 0.12	0.57 ± 0.25	**0.04**
Kep	2.81 ± 1.45	1.39 ± 1.23	0.39

Data are reported as mean ± standard deviation. Significative differences are represented in bold

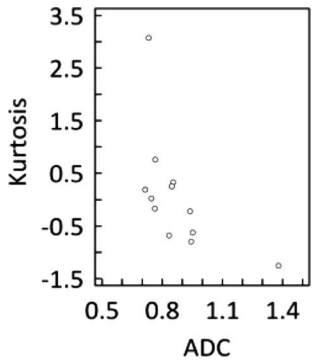

Fig. 6. A significant negative correlation between kurtosis and ADC was observed.

more patients, a significant association could be confirmed.

Regarding the role of DWI, ADC seemed to be ineffective in predicting CRT response, suggesting that tumor cellularity is not directly implicated in the response to therapy. On the reverse, the fact that pCR showed a lower kurtosis in comparison with PR and NR, support the observation that tumors with higher aggressiveness and poorer outcome have a higher heterogeneity [28].

Kurtosis and pMRI parameters showed no significant correlation, supporting the hypothesis that these biomarkers detect two distinct aspects of tumoral pathophysiology. Texture analysis is a marker of tissutal heterogeneity, instead pMRI is a marker of tumor vascularization. This could mean that heterogeneity and vascularization are not strictly related in case of rectal tumors, and they could play a separate role in defining the tumoral response to CRT.

Instead, a significant negative correlation was observed between kurtosis and ADC, suggesting that an increment in tumor cellularity, showed by an ADC reduction, is associated with an increased tumoral heterogeneity, likely due to intratumoral necrotic phenomena. Consequently, the lack of any predictive value

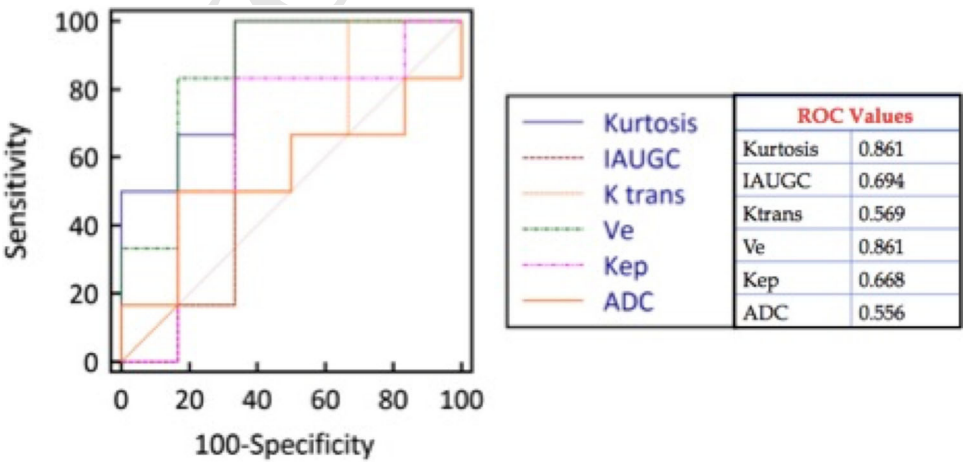

Fig. 7. Receiver operating characteristic (ROC) curves are shown analyzing the discriminatory power of baseline Kurtosis, ADC, and pMRI parameters to distinguish between pCR and PR + NR.

Journal : 261_ABDI Dispatch : 4-4-2016 Pages : 8
Article No. : 733 ☐ LE ☐ TYPESET
MS Code : ABDI ☑ CP ☑ DISK

of ADC seems pretty peculiar based on this correlation, and it could be the result of an insufficient statistical power secondary to the low number of patients analyzed.

Our study has several limitations which warrant discussion. Firstly, correlations between texture parameters, ADC, pMRI parameters, and tumoral response should be confirmed in larger studies with representative populations due to the limited number of patients in our preliminary study. Secondly, we did not analyze the incremental value of a multiparametric imaging approach (texture analysis + ADC + pMRI) and their combination on the prediction of tumoral response and patient outcome. Thirdly, a volumetric texture evaluation was not performed because the available software allowed only a single-slice evaluation. In addition, a correlation between our results and biological activity of the tumor was not performed because we did not evaluate biomolecular analysis of proteins expression of tumoral tissue, a marker of tumor aggressiveness. Finally, no follow-up evaluation was performed at the moment of the analysis, thus we did not evaluate the predictive value of these biomarkers on patient survival.

In conclusion, our preliminary results suggest that kurtosis derived from T2w images and Ve derived from pMRI have the potential to act as imaging biomarkers of tumoral response to neoadjuvant CRT in rectal cancer.

Acknowledgments. This study was funded by AIRC (Associazione Italiana per la Ricerca sul Cancro), Investigator Grant 2013/14129.

Compliance with ethical standards

Conflict of interest B. Ganeshan is a director, part-time employee, and shareholder of Feedback Plc (Cambridge, England, UK), company that develops and markets the TexRAD texture analysis algorithm described in this manuscript. The other authors declare that they have no conflict of interest.

Ethical approval All procedures performed in studies involving human participants were in accordance with the ethical standards of the institutional and/or national research committee and with the 1964 Helsinki declaration and its later amendments or comparable ethical standards.

References

1. van der Paardt MP, Zagers MB, Beets-Tan RG, Stoker J, Bipat S (2013) Patients who undergo preoperative chemoradiotherapy for locally advanced rectal cancer restaged by using diagnostic MR imaging: a systematic review and meta-analysis. Radiology 269:101–112
2. Taylor FG, Quirke P, Heald RJ, et al. (2011) Preoperative high-resolution magnetic resonance imaging can identify good prognosis stage I, II, and III rectal cancer best managed by surgery alone: a prospective, multicenter, European study. Ann Surg 253:711–719
3. Joye I, Deroose CM, Vandecaveye V, Haustermans K (2014) The role of diffusion-weighted MRI and (18)F-FDG PET/CT in the prediction of pathologic complete response after radiochemotherapy for rectal cancer: a systematic review. Radiother Oncol 113:158–165
4. Kim SH, Lee JM, Hong SH, et al. (2009) Locally advanced rectal cancer: added value of diffusion-weighted MR imaging in the evaluation of tumor response to neoadjuvant chemo- and radiation therapy. Radiology 253:116–125
5. Lambregts DM, Vandecaveye V, Barbaro B, et al. (2011) Diffusion-weighted MRI for selection of complete responders after chemoradiation for locally advanced rectal cancer: a multicenter study. Ann Surg Oncol 18:2224–2231
6. Jung SH, Heo SH, Kim JW, et al. (2012) Predicting response to neoadjuvant chemoradiation therapy in locally advanced rectal cancer: diffusion-weighted 3 Tesla MR imaging. J Magn Reson Imaging 35:110–116
7. Musio D, De Felice F, Magnante AL, et al. (2013) Diffusion-weighted magnetic resonance application in response prediction before, during, and after neoadjuvant radiochemotherapy in primary rectal cancer carcinoma. Biomed Res Int 2013:740195
8. Martens MH, Lambregts DM, Papanikolaou N, et al. (2014) Magnetization transfer ratio: a potential biomarker for the assessment of postradiation fibrosis in patients with rectal cancer. Invest Radiol 49:29–34
9. Lezoche E, Guerrieri M, Paganini AM, et al. (2005) Long-term results in patients with T2-3 N0 distal rectal cancer undergoing radiotherapy before transanal endoscopic microsurgery. Br J Surg 92:1546–1552
10. Serra-Aracil X, Mora-Lopez L, Alcantara-Moral M, et al. (2014) Transanal endoscopic surgery in rectal cancer. World J Gastroenterol 20:11538–11545
11. Hartley A, Ho KF, McConkey C, Geh JI (2005) Pathological complete response following pre-operative chemoradiotherapy in rectal cancer: analysis of phase II/III trials. Br J Radiol 78:934–938
12. O'Neill BD, Brown G, Heald RJ, Cunningham D, Tait DM (2007) Non-operative treatment after neoadjuvant chemoradiotherapy for rectal cancer. Lancet Oncol 8:625–633
13. Sebag-Montefiore D, Stephens RJ, Steele R, et al. (2009) Preoperative radiotherapy versus selective postoperative chemoradiotherapy in patients with rectal cancer (MRC CR07 and NCIC-CTG C016): a multicentre, randomised trial. Lancet 373:811–820
14. Peeters KC, Marijnen CA, Nagtegaal ID, et al. (2007) The TME trial after a median follow-up of 6 years: increased local control but no survival benefit in irradiated patients with resectable rectal carcinoma. Ann Surg 246:693–701
15. Lim JS, Kim D, Baek SE, et al. (2012) Perfusion MRI for the prediction of treatment response after preoperative chemoradiotherapy in locally advanced rectal cancer. Eur Radiol 22:1693–1700
16. Monguzzi L, Ippolito D, Bernasconi DP, et al. (2013) Locally advanced rectal cancer: value of ADC mapping in prediction of tumor response to radiochemotherapy. Eur J Radiol 82:234–240
17. Ng F, Ganeshan B, Kozarski R, Miles KA, Goh V (2013) Assessment of primary colorectal cancer heterogeneity by using whole-tumor texture analysis: contrast-enhanced CT texture as a biomarker of 5-year survival. Radiology 266:177–184
18. De Cecco CN, Ganeshan B, Ciolina M, et al. (2015) Texture analysis as imaging biomarker of tumoral response to neoadjuvant chemoradiotherapy in rectal cancer patients studied with 3-T magnetic resonance. Invest Radiol 50:239–245
19. Curvo-Semedo L, Lambregts DM, Maas M, et al. (2012) Diffusion-weighted MRI in rectal cancer: apparent diffusion coefficient as a potential noninvasive marker of tumor aggressiveness. J Magn Reson Imaging 35:1365–1371
20. Song I, Kim SH, Lee SJ, et al. (2012) Value of diffusion-weighted imaging in the detection of viable tumour after neoadjuvant chemoradiation therapy in patients with locally advanced rectal cancer: comparison with T2 weighted and PET/CT imaging. Br J Radiol 85:577–586
21. DeVries AF, Piringer G, Kremser C, et al. (2014) Pretreatment evaluation of microcirculation by dynamic contrast-enhanced magnetic resonance imaging predicts survival in primary rectal cancer patients. Int J Radiat Oncol Biol Phys 90:1161–1167
22. Attenberger UI, Pilz LR, Morelli JN, et al. (2014) Multi-parametric MRI of rectal cancer—do quantitative functional MR measurements correlate with radiologic and pathologic tumor stages? Eur J Radiol 83:1036–1043
23. Yeo DM, Oh SN, Jung CK, et al. (2015) Correlation of dynamic contrast-enhanced MRI perfusion parameters with angiogenesis and biologic aggressiveness of rectal cancer: Preliminary results. J Magn Reson Imaging 41:474–480

Journal : 261_ABDI | Dispatch : 4-4-2016 | Pages : 8
Article No. : 733 | ☐ LE | ☐ TYPESET
MS Code : ABDI | ☑ CP | ☑ DISK

24. Gollub MJ, Gultekin DH, Akin O, et al. (2012) Dynamic contrast enhanced-MRI for the detection of pathological complete response to neoadjuvant chemotherapy for locally advanced rectal cancer. Eur Radiol 22:821–831
25. Heald RJ, Ryall RD (1986) Recurrence and survival after total mesorectal excision for rectal cancer. Lancet 1:1479–1482
26. Dworak O, Keilholz L, Hoffmann A (1997) Pathological features of rectal cancer after preoperative radiochemotherapy. Int J Colorectal Dis 12:19–23
27. Miles KA, Ganeshan B, Hayball MP (2013) CT texture analysis using the filtration-histogram method: what do the measurements mean? Cancer Imaging 13:400–406
28. Ganeshan B, Abaleke S, Young RC, Chatwin CR, Miles KA (2010) Texture analysis of non-small cell lung cancer on unenhanced computed tomography: initial evidence for a relationship with tumour glucose metabolism and stage. Cancer Imaging 10:137–143

Journal : 261_ABDI | Dispatch : 4-4-2016 | Pages : 8
Article No. : 733 | ☐ LE | ☐ TYPESET
MS Code : ABDI | ☑ CP | ☑ DISK